

Impact Forces in the Simulation of Simultaneous Impacts and Contacts in Multibody Systems with Friction

Daniel Montralto Flickinger and Alan Bowling

Abstract—

This paper presents a method for determining impact forces associated with an abrupt velocity change when a free-flying body comes into contact with another body. Hard impact is considered where deformation of the impacting surfaces is negligible. The proposed approach uses a discrete algebraic model of impact in conjunction with moment and tangential coefficients of restitution (CORs) to develop a general impact law for determining post-impact velocities. This process depends on impulse-momentum theory, complementarity conditions, a principle of maximum dissipation, and the determination of impact and contact forces as well as post-impact accelerations. The proposed methodology also uses an energy-modifying COR to directly control the system's energy profile over time. The approach is illustrated on a planar bicycle-like structure.

I. INTRODUCTION

This paper presents a method for determining impact forces in simulation for systems of interconnected rigid bodies experiencing simultaneous *hard* impacts and contacts with consideration of Coulomb friction and energy consistency. The proposed method combines many elements, including: 1) discrete algebraic impact modeling, 2) impact and contact forces, 3) contact treated as successive impacts, 4) translational and rotational, normal and tangential CORs, 5) complementarity conditions, 6) maximum dissipation principle, 7) impact force minimization, 8) energetic and energy modifying CORs, and 9) event-based, adaptive numerical integration.

In this work a distinction is made between impact forces of short duration and contact forces of long duration, relative to the numerical integration step size. Here a discrete model of impact is used in order to study impact situations where surface deformation can be neglected. This approach also avoids the high-frequency vibrations created when stiff springs are used to model hard impacts [1]–[4].

In the next sections the overall integration scheme is discussed first, followed by the determination of impact and contact forces. Finally, an example of a planar bicycle-like structure with elliptical wheels is presented.

II. BACKGROUND

Discrete models can be classified as *differential* or *algebraic*. Differential approaches use an additional numerical integration in impulse space to capture phenomena occurring during the short duration impact event [5], [6]. In order to avoid the added computations, an algebraic approach is

developed here. The goal is to define enough equations to algebraically solve for the post-impact velocities. There are many ways to do this, see [1], [7], but the method proposed here is unique.

The classical approach towards addressing impact in discrete modeling is to examine the problem in terms of *impulsive forces* using impulse and momentum theory. An impulsive force results from integrating an impact force over a small time interval.

Impulsive forces result from integrating impact forces over the short duration of the impact event. Although it can be argued that impact forces appear to be infinite when examined at the large time scale of the numerical integration [8], they are assumed to be finite if examined at a small time scale.

The consideration of contact as successive impacts allows impact and contact to be modeled within the same framework so that simultaneous contacts and impacts can be addressed. This approach eliminates the need to remove generalized coordinates in order to enforce contact constraints, as is done in [9], which can be an arbitrary process [10]. It also allows contact points to easily alternate between *sticking* and *slipping* tangentially to the surface.

III. OVERVIEW OF NUMERICAL INTEGRATION

When considering systems of interconnected bodies, the simulation of contacts and impacts usually involves a numerical integration of the equations of motion:

$$A(\mathbf{q})\ddot{\mathbf{q}} + \mathbf{b}(\mathbf{q}, \dot{\mathbf{q}}) + \mathbf{g}(\mathbf{q}) = J^T(\mathbf{q}) \mathbf{F} + \mathbf{\Gamma} \quad (1)$$

where $\mathbf{q} \in \mathbb{R}^n$ contains the generalized/joint coordinates and $\dot{\mathbf{q}}$ and $\ddot{\mathbf{q}}$ contain their time derivatives, generalized speeds and accelerations. Terms $\mathbf{b} \in \mathbb{R}^n$, $\mathbf{g} \in \mathbb{R}^n$, $\mathbf{F} \in \mathbb{R}^m$, and $\mathbf{\Gamma} \in \mathbb{R}^n$ are the velocity, gravity, impact and/or contact, and other forces where $m \leq n$. Terms $J^T \in \mathbb{R}^{n \times m}$ and $A \in \mathbb{R}^{n \times n}$ are the Jacobian and inertia matrices respectively.

A common approach towards simulating discrete impacts is to stop the simulation at the start of the impact event, resolve the post-impact velocities, and restart it at the same time and position/orientation using the new velocities as an initial condition. However, if it is impractical to restart the simulation after each impact event, simply resetting the velocities does not work.

In order to illustrate this point consider numerically integrating (1) which must first be converted into two first order differential equations using the following change of variables

$$\dot{\mathbf{q}} = \mathbf{u} \quad \dot{\mathbf{u}} = \ddot{\mathbf{q}} \quad (2)$$

Daniel Montralto Flickinger and Alan Bowling at the Department of Mechanical and Aerospace Engineering, The University of Texas at Arlington, Arlington, TX 76019 USA bowling@uta.edu, daniel.flickinger@mavs.uta.edu

such that

$$\mathbf{x} = \begin{bmatrix} \mathbf{q} \\ \mathbf{u} \end{bmatrix} = \int_{\Delta t} \dot{\mathbf{x}} dt \quad (3)$$

$$\dot{\mathbf{x}} = \begin{bmatrix} \dot{\mathbf{q}} \\ \dot{\mathbf{u}} \end{bmatrix} = \begin{bmatrix} \mathbf{u} \\ A^{-1} (J^T \mathbf{F} + \mathbf{\Gamma} - \mathbf{b} - \mathbf{g}) \end{bmatrix}. \quad (4)$$

Consider an Euler numerical integration of $\dot{\mathbf{x}}$

$$\begin{bmatrix} \mathbf{q}(t_1) \\ \mathbf{u}(t_1) \end{bmatrix} = \begin{bmatrix} \mathbf{q}(t_0) + \Delta t \mathbf{u}(t_0) \\ \mathbf{u}(t_0) + \Delta t \dot{\mathbf{u}}(t_0) \end{bmatrix} \quad (5)$$

and at time t_2

$$\begin{bmatrix} \mathbf{q}(t_2) \\ \mathbf{u}(t_2) \end{bmatrix} = \begin{bmatrix} \mathbf{q}(t_1) + \Delta t \mathbf{u}(t_1) \\ \mathbf{u}(t_1) + \Delta t \dot{\mathbf{u}}(t_1) \end{bmatrix}. \quad (6)$$

Assume that at time t_0 two points impact, stick and do not rebound such that $\mathbf{q}(t_i) = \mathbf{q}(t_0)$ for all $i > 0$, implying that $\dot{\mathbf{q}}(t_0) = \mathbf{u}(t_0) = \mathbf{0}$. If the numerical integration is not interrupted at the impact event, then $\mathbf{q}(t_2) = \mathbf{q}(t_0)$ only if $\dot{\mathbf{u}}(t_0) = \mathbf{0}$. This is because $\dot{\mathbf{u}}(t_0)$ will be integrated up, resulting in a position/orientation change, unless it is also set equal to zero. Forcing the acceleration to equal zero motivates a solution for the contact forces

$$\mathbf{F}(t_0) + (JJ^T)^{-1} J(\mathbf{\Gamma}(t_0) - \mathbf{b}(t_0) - \mathbf{g}(t_0)) = \mathbf{0}. \quad (7)$$

In general, this approach is followed herein, except that usually the post-impact generalized speeds are not zero.

The adaptive event-based numerical integrator `ode45.m` in Matlab is used to solve this problem. In an event-based scheme, the integrator simulates the system up to the precise time that an impact occurs and stops. This allows the system states to be changed, and the integrator restarted; avoiding numerical problems caused by discontinuities. Detecting impact events kinematically becomes cumbersome, because contact is treated as a succession of impacts. However, the calculated contact or impact forces alone can be used to trigger events, allowing the integrator to proceed continuously if the contact state remains unchanged.

IV. IMPACT AND CONTACT FORCES

Determination of contact forces has been a widely used approach in impact and contact simulation [10]–[12]. The proposed approach is most similar to that in [13] which examined a Newton-Euler formulation for non-colliding contact at multiple points between several unconnected rigid bodies. The difference here is the examination of collisions involving impact and contact for systems of interconnected rigid bodies.

The goal is to determine the post-impact forces required to achieve desired post-impact accelerations, as discussed in Sec III. In order to accomplish this, it is necessary to make a notational distinction between impact and contact forces and accelerations. The contact and impact forces in the equations of motion (1) are expressed as

$$J^T \mathbf{F} = J^T P \begin{bmatrix} \mathbf{F}_p \\ \mathbf{F}_c \end{bmatrix} = \begin{bmatrix} J_p^T & J_c^T \end{bmatrix} \begin{bmatrix} \mathbf{F}_p \\ \mathbf{F}_c \end{bmatrix} \quad (8)$$

where $\mathbf{F}_p \in \mathbb{R}^p$ and $\mathbf{F}_c \in \mathbb{R}^c$ ($m = p + c \leq n$) contain impact and contact forces and P is a permutation matrix.

The following developments rely heavily on the dual nature of the impact Jacobian which expresses a relationship between forces and velocities [14]:

$$\boldsymbol{\vartheta} = \begin{bmatrix} \mathbf{v}_1 \\ \boldsymbol{\omega}_1 \\ \vdots \end{bmatrix} = \begin{bmatrix} \mathbf{v}_{t_1} \\ v_{n_1} \\ \boldsymbol{\omega}_{t_1} \\ \omega_{n_1} \\ \vdots \end{bmatrix} = J \dot{\mathbf{q}}, \quad \mathbf{F} = \begin{bmatrix} \mathbf{f}_{t_1} \\ \mathbf{f}_{n_1} \\ \mathbf{m}_{t_1} \\ \mathbf{m}_{n_1} \\ \vdots \end{bmatrix} \quad (9)$$

$$\dot{\boldsymbol{\vartheta}} = \dot{\boldsymbol{\vartheta}}_p + \dot{\boldsymbol{\vartheta}}_c = \dot{J}_p \dot{\mathbf{q}} + J_p \ddot{\mathbf{q}} + \dot{J} \dot{\mathbf{q}} + J \ddot{\mathbf{q}}. \quad (10)$$

The terms $\mathbf{v}_i \in \mathbb{R}^3$ and $\mathbf{f}_i \in \mathbb{R}^3$ are the translational velocity of, and force acting at the i^{th} impact point, while $\boldsymbol{\omega}_i \in \mathbb{R}^3$ and $\mathbf{m}_i \in \mathbb{R}^3$ are the rotational velocity of, and the moment acting on the body containing the i^{th} impact point. The ‘t’ and ‘n’ subscripts indicate forces, velocities, and accelerations normal and tangential to the impacting surface.

The tangential and normal components of the forces and accelerations are defined as

$$\mathbf{F}_p = \begin{bmatrix} \mathbf{f}_{pt_1}^T & \mathbf{f}_{pn_1} & \mathbf{m}_{pt_1}^T & \mathbf{m}_{pn_1} & \cdots \end{bmatrix}^T \quad (11)$$

$$\dot{\boldsymbol{\vartheta}}_p = \begin{bmatrix} \dot{\mathbf{v}}_{pt_1}^T & \dot{v}_{pn_1} & \dot{\boldsymbol{\omega}}_{pt_1}^T & \dot{\omega}_{pn_1} & \cdots \end{bmatrix}^T \quad (12)$$

likewise for other forces, velocities and accelerations.

The relations in (8), (9) and (11) define equivalent forces used to represent the complex set of forces occurring in the impact region. This set of forces is represented as a single resultant force acting at a reference point within the impact area and the sum of moments acting about the reference point.

Here it is assumed that $\dot{\boldsymbol{\vartheta}}_p$ is determined only by the impact forces. The relationship between $\dot{\boldsymbol{\vartheta}}_p$ and \mathbf{F}_p is found by considering impulses and momenta. The indefinite integration of (1) over a small time interval yields

$$A \dot{\mathbf{q}} + \mathbf{constant} = J_p^T \mathbf{p} \quad (13)$$

where $\mathbf{constant}$ contains the constants of integration. Differentiating (13) yields the impact forces

$$\dot{A} \dot{\mathbf{q}} + A \ddot{\mathbf{q}} = J_p^T \mathbf{F}_p. \quad (14)$$

V. DETERMINATION OF IMPACT FORCES

Before determining the impact forces, the velocities should be corrected to obtain the desired energy levels so that $\dot{\mathbf{q}}^*$ is used to minimize the impact forces. The constraints on the minimization enforce energy consistency using the *Work-Energy Theorem* [15],

$$T(\dot{\mathbf{q}}^*) - T(\dot{\mathbf{q}}(t)) = W_\epsilon = \int_t^{t+\epsilon} J_p^T \mathbf{F}_p(t) \cdot \dot{\mathbf{q}}(t) dt. \quad (15)$$

The integration variable can be changed using $d\mathbf{q} = \dot{\mathbf{q}} dt$ with a change of limits

$$T(\dot{\mathbf{q}}^*) - T(\dot{\mathbf{q}}(t)) = \int_{\mathbf{q}(t)}^{\mathbf{q}(t+\epsilon)} J_p^T \mathbf{F}_p(t) \cdot d\mathbf{q}. \quad (16)$$

However, over this small time interval \mathbf{q} is considered constant so it is not a function of t , and t is not a function of \mathbf{q} , therefore

$$\begin{aligned} T(\dot{\mathbf{q}}^*) - T(\dot{\mathbf{q}}(t)) &= \mathbf{J}_p^T (\mathbf{F}_p(t + \epsilon) \cdot \mathbf{q}(t + \epsilon) - \mathbf{F}_p(t) \cdot \mathbf{q}(t)) \\ &= \mathbf{J}_p^T \mathbf{F}_p(t + \epsilon) \cdot \mathbf{q}(t + \epsilon) \end{aligned} \quad (17)$$

since $\mathbf{F}_p(t) = \mathbf{0}$.

When all post-impact velocities are known the following problem is solved to minimize the impact forces

$$\begin{aligned} \min_{\dot{\vartheta}_p^*} \quad & \text{obj} := \mathbf{F}_p^T(t + \epsilon) (\mathbf{J}_p \mathbf{A}^{-1} \mathbf{J}_p^T) \mathbf{F}_p(t + \epsilon) \\ \text{subject to} \quad & T(\dot{\mathbf{q}}^*) - T(\dot{\mathbf{q}}(t)) = \mathbf{q}^T(t + \epsilon) \mathbf{J}_p^T \mathbf{F}_p(t + \epsilon) \\ & 0 \leq \mathbf{f}_{pn_i} . \end{aligned} \quad (18)$$

Knowing $\dot{\vartheta}_p^*$ and $\dot{\mathbf{q}}^*$ the impact forces are

$$\mathbf{F}_p(t + \epsilon) = (\mathbf{J}_p \mathbf{A}^{-1} \mathbf{J}_p^T)^{-1} \left(\dot{\vartheta}_p^* - \dot{\mathbf{J}}_p \dot{\mathbf{q}}^* + \mathbf{J}_p \mathbf{A}^{-1} \dot{\mathbf{A}} \dot{\mathbf{q}}^* \right) . \quad (19)$$

These forces are substituted back into the equations of motion, and used to calculate the post-impact accelerations. The integrator restarts with the new states, and the simulation proceeds to the next impact event.

VI. EXAMPLE

The bicycle system shown in Figure 1 is used here to illustrate the method developed in the previous sections. Gravity acts downward in the $-\mathbf{N}_2$ direction. Figure 1 also shows a wedge whose surface is parallel to vector \mathbf{A}_1 . A slender rod, body ‘B’, is pin connected to the two elliptical bodies, ‘C’ and ‘D’, at their mass centers; bodies ‘C’ and ‘D’ are identical. The mass center of the rod is located at point ‘B_o’ and the standard formulas for its moments of inertia are used. The standard moments of inertia for elliptical bodies are also used. The physical properties of the bicycle are given in Table I.

TABLE I

PHYSICAL PROPERTIES AND PARAMETERS FOR BICYCLE SIMULATIONS.

Figure	CPU time
2	700.34 seconds, (12 minutes)
3	580.34 seconds, (10 minutes)
4	1320.97 seconds, (22 minutes)

$$\begin{aligned} d_1 &= 0.5m & d_2 &= 1m & h &= 10m & L_1 &= 1m & m_B &= 1kg \\ m_C &= 2kg & m_D &= 2kg & \alpha &= 20^\circ & \mu_s &= 0.5 & \mu_d &= 0.25 \\ \text{Initial configuration } \mathbf{q}_o &= \{5m, 5m, 0^\circ, 0^\circ, 0^\circ\}^T \end{aligned}$$

A wedge of slope 20 degrees representing the ground is depicted as a gray region. The coefficient of restitution of the wedge is specified. The bicycle is drawn at the initial and final configurations, and at impact events. The plotted trajectory corresponds to the geometric center of the rigid bar coupling the two masses.

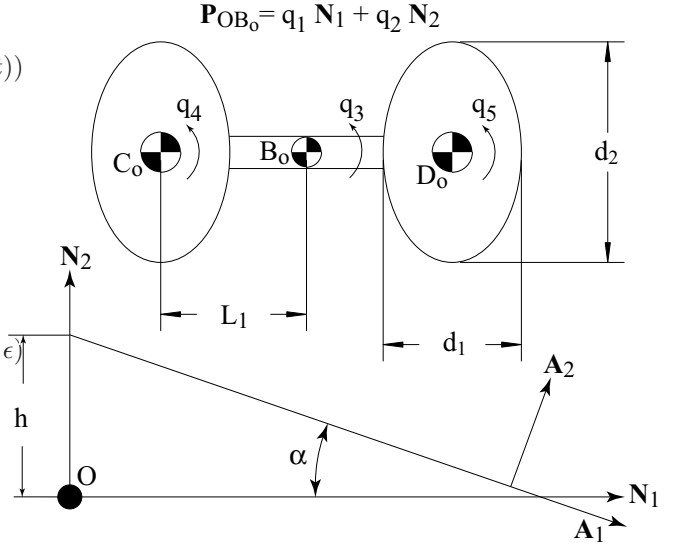


Fig. 1. Bicycle-like System. The “wheels” are elliptical and are pin-connected to the bar through their mass centers, points C_o and D_o . Their rotation is measured by the generalized coordinates q_4 and q_5 . The position vector \mathbf{P}_{OB_o} points from ‘O’ to ‘B_o’.

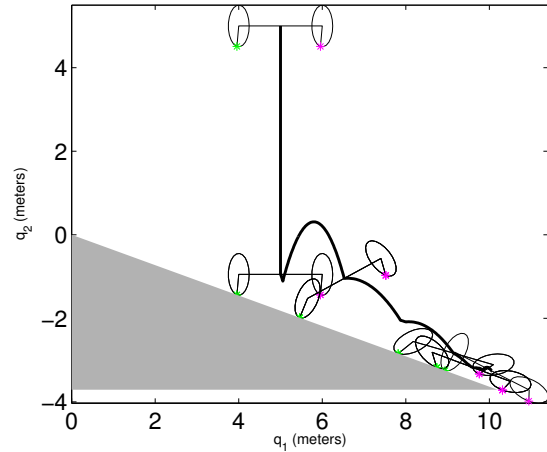


Fig. 2. Bicycle trajectory with a coefficient of restitution of 0.75

A. Coefficient of Restitution of 0.75

The COR is set to 0.75 to approximate an elastic surface. The parameter $e_* = 0.5$ enforces that at least half of all kinetic energy is lost at each impact.

The trajectory is plotted in Figure 2. The mechanism bounces several times down the wedge, traveling much further than in later tests with lower CORs.

The impact and contact forces are given in Figure 5. The peaks from each impact are shown. The total and kinetic energy are plotted in Figure 5. At each impact, approximately half of the kinetic energy is lost. The energy is largely regained during the ballistic phases as the bicycle travels down the wedge. After several bounces, the mechanism

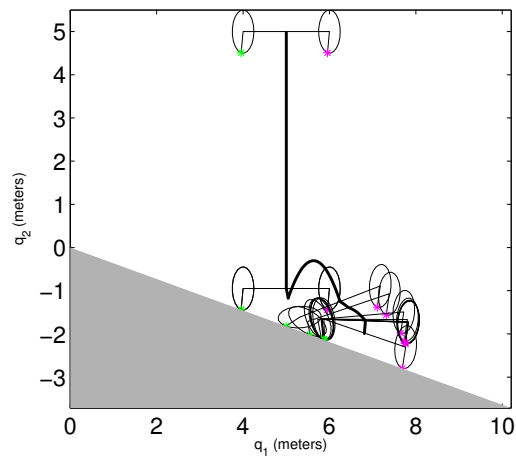


Fig. 3. Bicycle trajectory with a coefficient of restitution of 0.5

transitions from rebounding impact to rolling contact. This occurs after approximately 3.5 seconds. The forces given in Figure 5 chatter while in rolling contact, hence the solid regions. The chattering is caused by a combination of using a rough approximation of the contact points between the ground and the ellipse shaped wheels of the mechanism, and coarse integrator tolerances set in an effort to reduce computation time.

B. Coefficient of Restitution of 0.5

The simulation is run with a COR decreased to 0.5. The resulting trajectory is shown in Figure 3. The mechanism bounces fewer times than in the previous example. In addition, the transition to rolling contact occurs sooner.

The impact and contact forces are given in Figure 6. The total and kinetic energy is plotted in Figure 6c. Chattering in the contact forces is again present after the transition of the mechanism from impact to rolling contact.

C. Coefficient of Restitution of 0.25

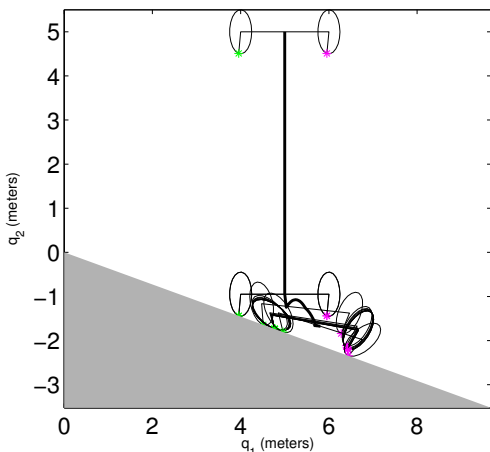


Fig. 4. Bicycle trajectory with a coefficient of restitution of 0.25

The coefficient of restitution is lowered to 0.25, simulating a soft or sandy surface. The resulting trajectory is given in Figure 4a. After the initial impact, the mechanism slides and rolls, coming to rest at a short distance down the wedge. The impact and contact forces, and energy are plotted in Figure 7b. The chattering during rolling contact is present, as in the previous examples. The magnitudes of the impact forces increase as the COR decreases, as more energy is lost to impact.

VII. CONCLUSIONS

This paper explains the development of a multibody impact and contact simulation, focusing on the determination of impact forces considering hard contact. The proposed methodology was illustrated on a planar bicycle-like structure, showing energy consistency and the transition from rebounding impact to rolling continuous contact. The simulation presented here handles discontinuities in velocities and acceleration due to impact by stopping and restarting the integration of the equations of motion with updated state data.

The results from the planar bicycle simulation show that this method can handle impact, contact, slipping, and rolling in a planar environment. Improvements can be made in eliminating chatter in the forces and accelerations under continuous contact. Future work includes expanding the simulation to handle impact and contact in three dimensional space, and simulating both passive and actuated legged mechanisms.

ACKNOWLEDGMENTS

This work was supported by NSF Grant #IIS-0238487. Any opinions, findings, and conclusions or recommendations expressed in this publication are those of the author(s) and do not reflect the views of the National Science Foundation.

REFERENCES

- [1] Gilardi, G., and Sharf, I., 2002. "Literature survey of contact dynamics modeling". *Mechanism and Machine Theory*, **37** (10) March , pp. 1213–1239.
- [2] Lankarani, H. M., and Nikravesh, P. E., 1990. "A contact force model with hysteresis damping for impact analysis of multibody systems". *Journal of Mechanical Design, Transactions of the ASME*, **112** September , pp. 369 – 376.
- [3] Gonthier, Y., Mcphee, J., Lange, C., and Piedbœuf, J., 2004. "A regularized contact model with asymmetric damping and dwell-time dependent friction". *Multibody System Dynamics*, **11** (3) April , pp. 209–233.
- [4] Flores, P., Ambròsio, J., and Claro, J. P., 2004. "Dynamic analysis for planar multibody mechanical systems with lubricated joints". *Multibody System Dynamics*, **12** (1) August , pp. 47–74.
- [5] Stronge, W. J., 1991. "Friction in collisions: Resolution of a paradox". *Journal of Applied Physics*, **69** January , pp. 610–612.
- [6] Stronge, W. J., 2000. *Impact Mechanics*. Cambridge University Press. pp. 173-200.
- [7] Brogliato, B., ten Dam, A., Paoli, L., Génot, F., and Abadie, M., 2002. "Numerical simulation of finite dimensional multibody nonsmooth mechanical systems". *Applied Mechanics Reviews*, **55** (2) March , pp. 107–149.
- [8] Glocker, C., 2006. "An introduction to impacts". In *Nonsmooth Mechanics of Solids*, vol. 485 of *CISM Courses and Lectures*. Springer-Verlag, Wien, New York, pp. 45–102.

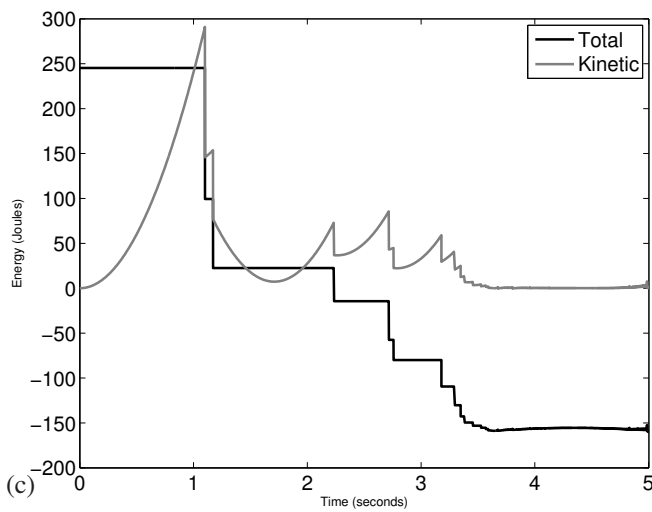
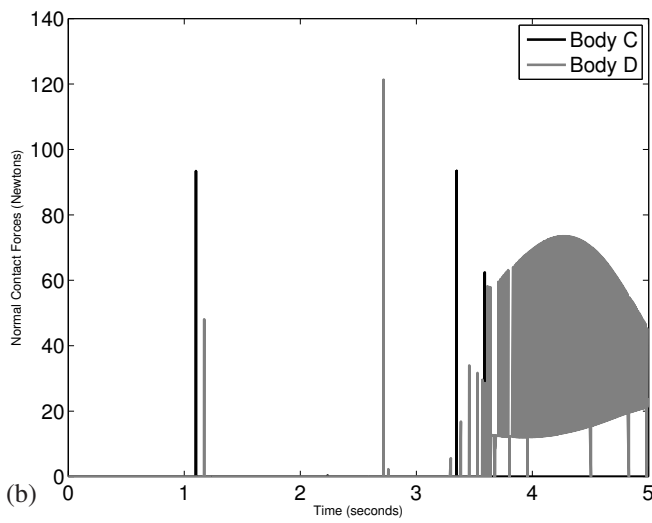
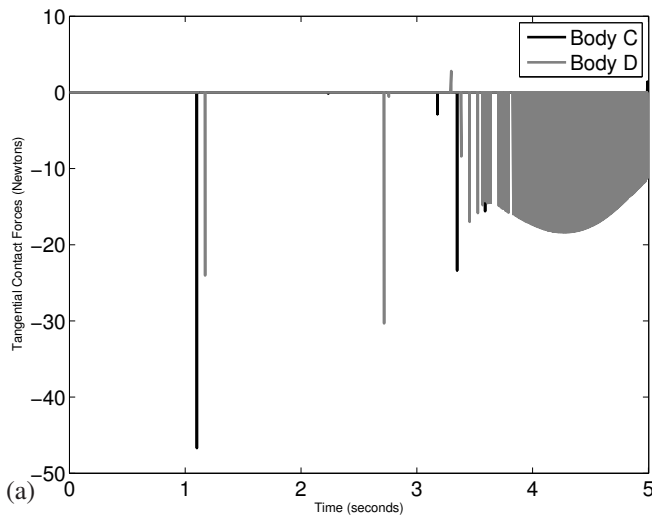


Fig. 5. Bicycle (a) tangential contact/impact forces, (b) normal contact/impact forces, and (c) energy with a coefficient of restitution of 0.75

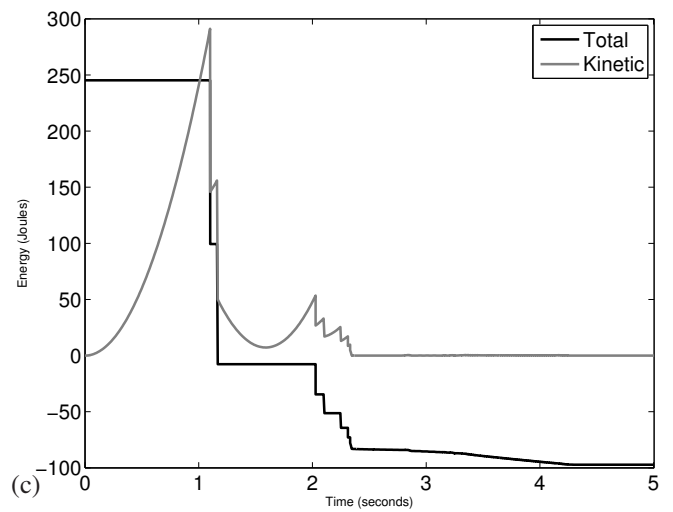
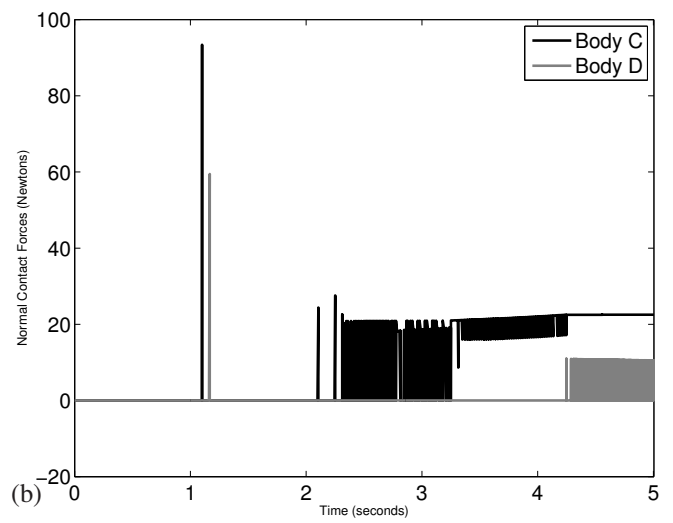
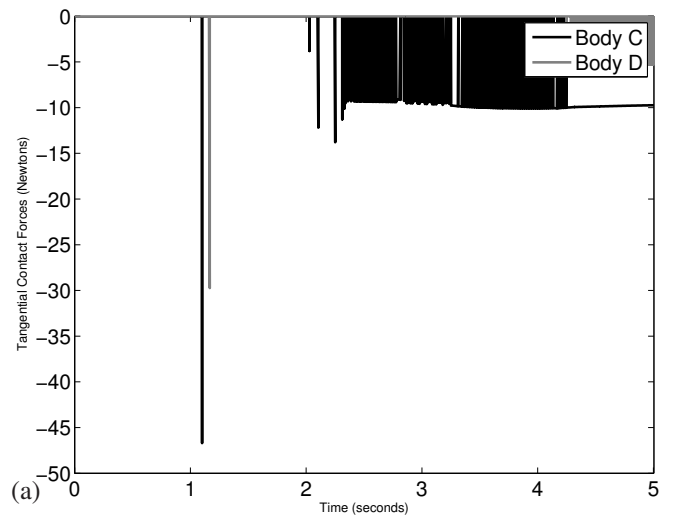


Fig. 6. Bicycle (a) tangential contact/impact forces, (b) normal contact/impact forces, and (c) energy with a coefficient of restitution of 0.5

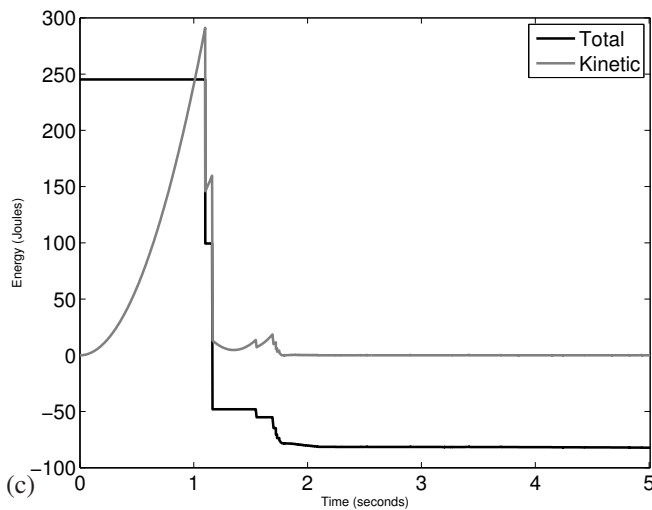
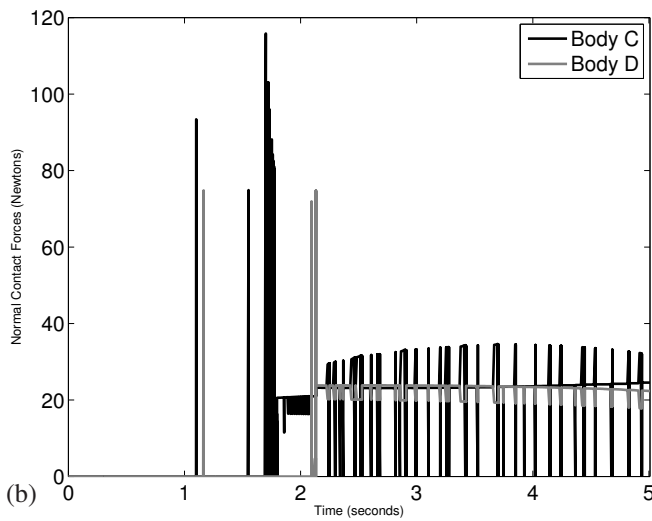
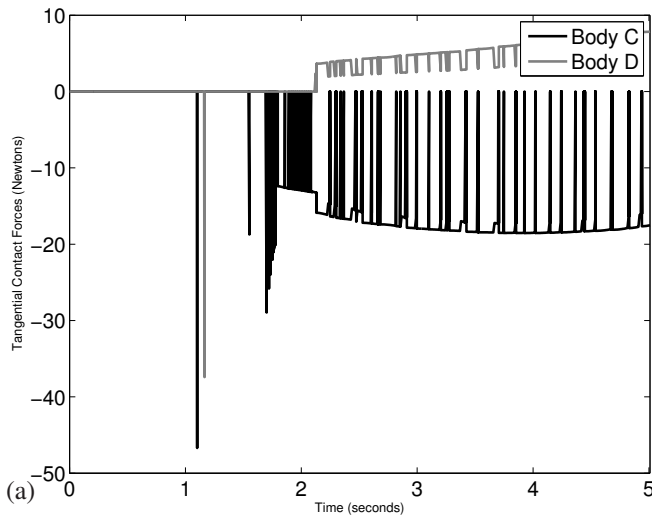


Fig. 7. Bicycle (a) tangential contact/impact forces, (b) normal contact/impact forces, and (c) energy with a coefficient of restitution of 0.25

[9] Gillespie, R. B., Patoglu, V., Hussein, I. I., and Westervelt, E. R., 2005. "On-line symbolic constraint embedding for simulation of hybrid dynamical systems". *Multibody System Dynamics*, **14** (3-4) November , pp. 387-417.

[10] Pfeiffer, F., and Glocker, C., 1996. *Multibody Dynamics with Unilateral Contacts*. Wiley Series in Nonlinear Science. John Wiley & Sons, Inc.

[11] Baraff, D., 1989. "Analytical methods for dynamic simulation of non-penetrating bodies". *Computer Graphics*, **23** (3) July , pp. 223-232.

[12] Glocker, C., and Studer, C., 2005. "Formulation and preparation for numerical evaluation of linear complementarity systems in dynamics". *Multibody System Dynamics*, **13** (4) May , pp. 447-463.

[13] Sharf, I., and Zhang, Y., 2006. "A contact force solution for non-colliding contact dynamics simulation". *Multibody System Dynamics*, **16** (3) October , pp. 263-290.

[14] Craig, J. J., 1989. *Introduction to Robotics: Mechanics and Control*, second ed. Addison-Wesley Publishing Company.

[15] Baruh, H., 1999. *Analytical Dynamics*, 1st ed. WCB MacGraw-Hill.